HHS Public Access

Author manuscript

FASEB J. Author manuscript; available in PMC 2022 February 26.

Published in final edited form as:

FASEB J. 2020 January ; 34(1): 619–630. doi:10.1096/fj.201901490RR.

Plasmin inhibition by bacterial serpin: implications in gum disease

Alicja Sochaj-Gregorczyk[*,1], **Miroslaw Ksiazek**[*,†,‡,1,2], **Irena Waligorska**[†], **Anna Straczek**[†], **Malgorzata Benedyk**[†], **Danuta Mizgalska**[†], **Ida B. Thøgersen**[§], **Jan J. Enghild**[§], **Jan Potempa**[†,‡]

[*]Malopolska Center of Biotechnology, Jagiellonian University, Krakow, Poland

[†]Department of Microbiology, Faculty of Biochemistry, Biophysics, and Biotechnology, Jagiellonian University, Krakow, Poland

[‡]Department of Oral Immunology and Infectious Diseases, University of Louisville School of Dentistry, Louisville, KY, United States

[§]Interdisciplinary Nanoscience Center (iNANO) and the Department of Molecular Biology, Aarhus University, Aarhus, Denmark

Abstract

Tannerella forsythia is a periodontopathogen that expresses miropin, a protease inhibitor in the serpin superfamily. In this study, we show that miropin is also a specific and efficient inhibitor of plasmin; thus it represents the first proteinaceous plasmin inhibitor of prokaryotic origin described to date. Miropin inhibits plasmin through the formation of a stable covalent complex triggered by cleavage of the Lys^{368}-Thr^{369} (P2-P1) reactive site bond with a stoichiometry of inhibition of 3.8 and an association rate constant (k_{ass}) of 3.3×10^5 $M^{-1}s^{-1}$. The inhibition of the fibrinolytic activity of plasmin was nearly as effective as that exerted by α_2-antiplasmin. Miropin also acted *in vivo* by reducing blood loss in a mice tail bleeding assay. Importantly, intact *T. forsythia* cells or outer membrane vesicles, both of which carry surface-associated miropin, strongly inhibited plasmin. In intact bacterial cells, the antiplasmin activity of miropin protects envelope proteins from plasmin-mediated degradation. In summary, in the environment of periodontal pockets, which are bathed in gingival crevicular fluid consisting of 70% of blood plasma, an abundance of *T. forsythia* in the bacterial biofilm can cause local inhibition of fibrinolysis, which could have possible deleterious effects on the tooth-supporting structures of the periodontium.

Keywords

plasmin; periodontitis; *Tannerella forsythia* ; serpin; fibrinolysis

[2]Corresponding author: Department of Microbiology, Faculty of Biochemistry, Biophysics and Biotechnology, Jagiellonian University ul. Gronostajowa 7, 30-387 Krakow, Poland, Tel: (+48) 12-664-69-02; Fax: (+48) 12-664-69-02, ksiazek.miroslaw@gmail.com.

[1]Equally contributed first author

AUTHOR CONTRIBUTIONS

M. Ksiazek and J. Potempa designed research; J. J. Enghild, and M. Ksiazek analyzed data; A. Sochaj520 Gregorczyk, M. Ksiazek, I. Waligorska, A. Straczek, M. Benedyk-Machaczka, and I. B. Thøgersen performed 521 research; A. Sochaj-Gregorczyk, M. Ksiazek, and J. Potempa wrote the paper; D. Mizgalska contributed 522 *T. forsythia* miropin deletion mutant.

INTRODUCTION

The plasminogen activation system plays essential roles in blood clot dissolution, wound healing, cell migration, tissue formation and regeneration, angiogenesis, and embryogenesis, as well as in the initiation and resolution of inflammatory reactions (1). To a large extent, these functions depend on the fibrin mesh generated via the coagulation cascade, which provides a scaffold for the remodeling and restoration of damaged tissue architecture by inflammatory cells (2), and this process requires very precise control of plasmin activity.

Plasmin is formed from plasminogen, its inactive precursor that is produced by the liver and circulates in plasma at a concentration of 1.5–2 μM (3). Only plasminogen bound to fibrin or immobilized on the cell surface, but not soluble zymogen, can be proteolytically activated under pathophysiological conditions by tissue plasminogen activator (tPA) and urokinase plasminogen activator (uPA) (4). Active plasmin is composed of two polypeptide chains that are joined by a disulfide bridge: a heavy chain (~60 kDa), which contains Kringle domains responsible for interactions with lysine residues on protein receptors, and a light chain (23 kDa) that includes a serine protease domain (1). *In vivo*, plasminogen activation via tPA and uPA is regulated by the PAI-1 and PAI-2 serpins, while the activity of soluble activated plasmin, but not fibrin- or receptor-bound plasmin, is strictly controlled by the serpin, α_2-antiplasmin and pan-proteinase inhibitor, α_2-macroglobulin (5, 6).

Another important function of fibrin deposits is to trap bacteria to prevent their spread (7). Therefore, it is no surprise that bacterial pathogens evolved strategies not only to avoid entrapment in the fibrin mesh but also to use the powerful proteolytic activity of plasmin to their own advantage. These strategies include direct activation of plasminogen via streptokinases produced by group A, C, and G streptococci, staphylokinase produced by *Staphylococcus aureus*, and the Pla protease expressed by *Yersinia pestis* (7, 8). A more universal approach for hijacking the host plasmin system is to express plasmin(ogen) receptors on the bacterial cell surface, and such receptors can be either specialized proteins or glycolytic enzymes that are released to the bacterial surface (9). These receptors bind plasminogen, facilitate its activation, and protect surface-bound plasmin from inactivation. In this way, bacteria acquire the pericellular proteolytic activity necessary for the dissemination and/or deterrence of host immune system attacks (7).

In humans, a rare (1 out of 1 million births) congenital plasminogen deficiency, referred to as type 1 plasminogen deficiency or hypoplasminogenemia, is defined by reduced levels of functional plasminogen in the circulation and is clinically manifested by mucous membrane thickening (10). The gingival mucosa is the site most often involved in the development of ligneous periodontitis characterized by extensive alveolar bone resorption and eventual tooth loss (11). Furthermore, antifibrinolytic therapy based on the use of tranexemic acid to block the binding of plasminogen to fibrin can occasionally lead to progressive periodontitis (12). These observations suggest that plasmin(ogen) is essential for maintaining periodontium homeostasis in humans (as it is in mice), where it is crucial for preventing the spontaneous development of periodontitis (13).

Chronic periodontitis, the most severe form of gum disease, involves chronic inflammation that results in the erosion of tooth-supporting tissues, including the periodontal ligament and the alveolar bone. It affects up to 50% of the adult population worldwide and is the major cause of tooth loss (14). To make matters worse, periodontitis is clinically and epidemiologically associated with multiple systemic diseases, including atherosclerotic cardiovascular disease (15), diabetes (16, 17), adverse pregnancy outcomes (18), chronic kidney disease (19), aspiration pneumonia (20, 21), rheumatoid arthritis (22), and neurodegenerative diseases (23).

Although chronic periodontitis is driven by a polymicrobial biofilm on the tooth surface below the gum line, species such as *Porphyromonas gingivalis*, *Treponema denticola*, and *Tannerella forsythia* play the most important roles in disease initiation and its progression to tooth loss (24). Colonization of bacterial biofilms by *P. gingivalis* not only directly stimulates a local inflammatory reaction, it also leads to a restructuring of the biofilm composition to favor dysbiotic inflammophilic (= loving or attracted to inflammation) pathobionts, which have evolved to not only endure inflammation but also to take advantage of it. (25). Neutrophils and macrophages, in futile attempts to eliminate the invaders, release copious amounts of proinflammatory factors that act together with cytokines released by other cells to drive the chronic inflammation-driven disintegration of the tooth-supporting structures (26, 27).

Except for *T. denticola*, which expresses two plasminogen-binding proteins (28), the other major periodontal pathogens do not capture nor activate plasminogen. Apparently, both *P. gingivalis* and *T. forsythia* rely on a broad array of secreted, cell surface-associated proteases for deterring, corrupting or hijacking the host immune system to their own advantage (29, 30). Surprisingly, in addition to several proteases, *T. forsythia* also expresses a serpin called miropin, a very potent, broad-specificity protease inhibitor (31, 32). Here, we show that soluble miropin and miropin associated with intact bacteria or outer membrane vesicles can very efficiently inhibit plasmin via the formation of a covalent complex. By contrast, miropin could not inhibit thrombin activity, nor did it exert any effect on plasma clotting dynamics. Importantly, miropin inhibited the fibrinolytic activity of plasmin in whole human plasma and was effective at reducing blood loss in an *in vivo* mouse model. To our knowledge, miropin is the first proteinaceous plasmin inhibitor found in prokaryotes that protects bacterial surface proteins from damage by plasmin.

MATERIALS AND METHODS

Materials, enzymes, and inhibitors

A rabbit polyclonal anti-miropin antibody was generated by Kaneka Eurogentec S.A. (Seraing, Belgium) using recombinant miropin as an antigen. Human plasmin, α_2-antiplasmin (α_2AP), and α_2-macroglobulin (α_2M) were from Athens Research & Technology, Inc. (Athens, GA, USA). Human thrombin was purchased from Haematologic Technologies, Inc. (Essex Junction, VT, USA). Plasmin was titrated with α2M, and its active concentration was determined using 4-nitrophenyl 4-guanidinobenzoate active site-titrated porcine trypsin. Therefore, the concentrations of plasmin used in this work refer not to

protein concentration, but to the concentration of active enzyme. All other reagents, if not mentioned otherwise, were from Sigma-Aldrich (St. Louis, MO, USA).

Bacterial growth and culture fractionation

WT and Δmiropin (5 μg/ml chloramphenicol in medium) strains of *T. forysthia* ATCC 43037 were grown until they reached mid-exponential phase (OD_{600} 0.4–0.6) or early stationary growth phase (OD_{600} 1.2–1.5), as described previously (31, 33). For *T. forsythia* culture partitioning, 25 ml *T. forsythia* (WT and Δmiropin) culture was supplemented with cOmplete Mini, EDTA-free protease inhibitor cocktail (Roche, Basel, Switzerland) at a 1× final concentration. Next, the *T. forsythia* cultures were fractionated into whole cells (WC), a "cell envelope" fraction (CE) containing the outer and inner membrane and the peptidoglycan, and the outer membrane vesicles (OMVs), as described previously (31, 34), but using TNC (50 mM Tris, 150 mM NaCl, 5 mM $CaCl_2$, pH 7.5) instead of PBS.

Expression and purification of recombinant proteins

$Miropin^{K368A}$ was generated by modifying the miropin-encoding plasmid pGEX-6P-1 with the QuikChange Lightning Site-Directed Mutagenesis Kit (Agilent, Santa Clara, CA, USA) using the oligonucleotides MK171 (5'-CCGTAGAAATGGTAGCAACGTCATCCCCCTC-3') and MK173 (5'-GAGGGGGATGACGTTGCTACCATTTCTACGG-3'). Tag-free homogenous recombinant proteins were obtained via an *Escherichia coli* expression system and affinity (glutathione-Sepharose) and size-exclusion chromatography (HiLoad 16/60 Superdex 75 pg), as described previously (31).

Plasmin inhibition

Human plasmin (40 or 0.5 nM) was mixed with increasing concentrations of miropin in assay buffer (0.1 M Tris, 150 mM NaCl, 5 mM $CaCl_2$, 0.02% NaN_3, pH 7.5) or with increasing volumes of *T. forsythia* WC and OMV fractions in assay buffer with 0.05% Pluronic F-127 in the wells of a microtitration plate (total volume 100 μl). After 15 or 30 min of incubation at 37 °C, 100 μl of 120 or 200 μM Boc-QAR-AMC substrate solution, respectively, was added, and the enzymatic hydrolysis of the substrate was monitored at 37 °C via fluorescence measurement (exc/em = 380/460 nm) with a SpectraMax Gemini XS microplate reader (Molecular Devices, San Jose, CA, USA). The residual activity was plotted as a function of the miropin:plasmin molar ratio or volumes of *T. forsythia* fractions. The stoichiometry of inhibition (SI) was defined as the value where the linear curve fitted to the data points crossed the x-axis. Alternatively, 10 ng plasmin was mixed in assay buffer with 2-fold serial dilutions of the WC and OMV fractions in a total volume of 20 μl. After incubation for 30 min at 37 °C, the samples were left for 5 min at RT and then subjected to Western blot analysis using miropin antibodies.

Progress curve analysis

The association rate constant (k_{ass}) was determined as described previously (31) by measuring the plasmin activity in assay buffer in the presence of increasing miropin

concentrations (0–500 nM), as described above. Plasmin was used at final concentrations of 1 nM, and the K_M for substrate turnover by plasmin was determined at 46 μM.

SDS-PAGE analysis and Western blotting

Samples were resolved via 10% or 18% (only for the reactive site determination) SDS-PAGE (T:C ratio 33:1) using a Tris-HCl/Tricine buffer system under reducing or non-reducing (without 5% w/v DTT) conditions (35). For the Western blot analysis, resolved proteins were subsequently electrotransferred (1 h/100 V at 4 °C in 25 mM Tris, 192 mM glycine, 20% methanol) onto 0.22 μm pore-size PVDF membranes and blocked overnight in blocking solution (TTBS, 20 mM Tris, 0.5 M NaCl, 0.1% Tween-20; pH 7.5) with 5% (w/v) skim milk. Next, the membranes were probed with a 1:1,000 dilution (0.6 μg/ml) of the anti-miropin antibody in blocking solution for 1 h, washed four times with TTBS, and then incubated for 1 h with a 1:15,000 dilution of an HRP-conjugated goat anti-rabbit polyclonal secondary antibody. Development was performed using the ECL Western blotting substrate kit (Pierce, Thermo Scientific, Waltham, MA, USA).

Covalent complex detection

To detect covalent plasmin-miropin complexes, increasing concentrations of plasmin (0–2.4 μM) were incubated in assay buffer (0.1 M Tris, 150 mM NaCl, 5 mM $CaCl_2$, 0.02% NaN_3, pH 7.5) with 4.8 μM miropin for 15 min at 37 °C in a total volume of 20 μl, and the proteins were then resolved via SDS-PAGE. The identities of the proteins in the bands of interest were determined via mass spectroscopy as described previously (31).

Determination of the cleavage sites in the Miropin reactive center loop (RCL)

Miropin (12 μM) and plasmin (3 μM) were mixed in a total volume of 20 μl in assay buffer and incubated for 15 min at 37 °C. The mixtures were resolved on 18% gels and electrotransferred onto a PVDF membrane (Bio-Rad, Hercules, CA, USA). The N-terminal sequences of stained peptides with a molecular weight of ~4.5 kDa were obtained via automated Edman degradation using a Procise 494HT amino acid sequencer (Applied Biosystems, Carlsbad, CA, USA), as described previously (31).

Determination of clotting time

Human blood plasma (25 μl) containing sodium citrate as an anticoagulant was mixed with miropin (final concentration: 10 μM) or assay buffer (control), and incubated for 30 min at 37 °C. Next, 25 μl Thromboplastin LI Reagent or APTT Si L Minus Reagent containing 25 mM $CaCl_2$ and prothrombin time (PT) or activated partial thromboplastin time (APTT), respectively, were added to the samples. The clotting time was measured using C-2 dual channel coagulometer and the HEM-AN LITE software (Helena Biosciences, Gateshead, United Kingdom).

Fibrinolytic turbidity assay

To form fibrin clots, 10 μl thrombin (100 U/ml) and 90 μl fibrinogen (1 mg/ml) or 10% human plasma in 25 mM Tris, pH 7.5, were mixed in the wells of microplates and then incubated for 30 min at RT. Next, 25 μl buffer only or inhibitor solution (antiplasmin or

miropin or miropin^{K368A}) was added to the clots, and the contents of the wells were mixed. Finally, 25 µl buffer (25 mM Tris, 0.05% Pluronic F-127) or plasmin solution (0.1 or 0.05 µM, respectively) was added. The fibrinolytic activity was measured for 1.5 h as a decrease in the absorbance at 350 nm. In this experiment and in the supplementation of antiplasmin-deficient plasma, the amounts of active inhibitor in the miropin and α_2AP preparations were determined via titration using active site-titrated plasmin. The concentration of the K368A mutant protein was calculated based on the protein content.

Proteolytic cell envelope degradation

The protein concentrations in the CE fractions isolated from WT and Δmiropin *T. forsythia* were determined via BCA assays strictly according to the manufacturer's instructions. CE suspension (50 µl) at concentration 1.8 mg/ml in assay buffer with Pluronic F-127 was pipetted into wells of 96-well clear microplates. Next, 25 µl assay buffer or a 0.4 µM solution of recombinant miropin or its inactive variant K368A in assay buffer was added followed by addition of 25 µl of 0.4 µM solution of human plasmin in assay buffer. Assay buffer without plasmin was used as a negative control. Time-dependent degradation of the CE proteins was monitored via measurement of the absorbance at 578 nm, as described previously (36).

Animal care and mouse tail vein bleeding model

All animal experimental procedures were performed according to the guidelines of the Institutional Animal Care and Use I Regional Ethics Committee on Animal Experimentation, Krakow, Poland (Decision No. 249/2017). Eight-week-old specific pathogen-free (SPF) female C57BL/6 mice were purchased from The Jackson Laboratory (USA). Mice were housed under standard conditions within the animal care facility at the Jagiellonian University, Krakow, in positively-ventilated microisolator cages, fed a standard laboratory diet, and allowed water *ad libitum*. Before the experimental procedures, the mice were sedated via intraperitoneal injection of a mixture of ketamine (22 mg/kg; VetaKetam, Vet-Agro, Poland) and xylazine (2 mg/kg; Sedasin, Biowet, Poland). While under anesthesia, the mice were intravenously injected (tail vein) with 100 µl of a solution containing 15 nmol of active miropin or aprotinin or 100 µl PBS, and the tail excision was performed 2 min later for each mouse. Blood loss was measured by weighing the blood collected into pre-weighed 288 Eppendorf tubes. After the procedure, all mice were euthanized via cervical dislocation. The procedure was 289 repeated in three independent experiments.

Inhibition of SK-activated plasmin

The activity of streptokinase (SK)-activated plasmin in human plasma was determined with human fibrinogen (Merck KGaA, Darmstadt, Germany) as the substrate following a previously described method with one modification (37). Increasing concentrations of recombinant miropin were added to mixtures containing SK-activated plasmin. Alternatively, after addition of recombinant miropin, samples were subjected to Western 297 blot analysis using miropin antibodies. The k_{ass} of SK-activated plasminogen in human antiplasmin-deficient 298 plasma was determined as described above using inhibition progress curves.

Supplementation of antiplasmin-deficient plasma

Human α_2AP-deficient plasma (ANIARA, West Chester, OH, USA) was supplemented with human antiplasmin or miropin (WT or K368A) to reach final concentrations equivalent to 1 μM active inhibitor. In the wells of microtiter plates, plasmin (10 nM) in assay buffer containing Pluronic F-127 was mixed with increasing volumes of plasma to reach a final volume of 100 μl followed by incubation for 30 min at 37 °C. Next, 100 μl of 0.2 mM substrate (Boc-QAR-AMC) solution was added, and the proteolytic activity was measured as the 307 fluorescence increase (exc/em = 380/460 nm).

RESULTS

Miropin is a specific plasmin inhibitor

Unique to serpins, miropin inhibits serine and cysteine proteases of various specificities (trypsin, elastase, subtilisin, and papain) using at least three reactive sites (Val*Lys*Thr*Ser) within the RCL (31, 32). Its 315 inhibition of trypsin at the Lys-Thr active site prompted us to investigate the ability of miropin to inhibit thrombin and plasmin, the key proteases in the coagulation and fibrinolysis cascades, respectively. At a 10-molar excess, miropin totally abrogated plasmin activity but had no effect on the amidolytic activity of thrombin on a synthetic substrate (Fig. 1A). It also appears that miropin does not inhibit other clotting factors since it did not affect PT and APTT even at a concentration of 10 μM (Fig. 1B). Together, these results indicate that miropin targets plasmin but none of the coagulation factors (thrombin, VIIa, IXa, Xa, XIa, and XIIa); thus its specificity is limited to clotting factors with Lys-Xaa peptide bonds.

Miropin inhibited plasmin in a concentration-dependent manner with a stoichiometry of inhibition (SI) of 3.8 (Fig. 2A) and a second-order association rate constant (k_{ass}) of 3.3×10^5 M^{-1} s^{-1}, as determined via progresscurve analysis (Fig. 2B). Under the same experimental conditions, human α_2-antiplasmin (α_2AP) targeted plasmin with a SI of 1.1 and a k_{ass} of 1.3×10^6 M^{-1} s^{-1} (data not shown). Importantly, miropin effectively inhibited both the amidolytic and fibrinolytic activities of plasmin. In this assay, 0.4 μM miropin slowed down the solubilization of a fibrin clot by plasmin with a level of effectiveness comparable to that of α_2AP at the same concentration. At 1.6 μM, miropin totally abrogated the clot dissolving ability of plasmin (Fig. 2C). Importantly, a miropin mutant with a substitution of the reactive site Lys residue with an Ala residue (miropin^{K368A}) had no effect, even at high concentrations. This result unambiguously rules out any other mode 331 of interference in clot resolution except for inhibitory complex formation.

A unique feature of protease inhibition by serpins is the formation of covalent complexes in which the targeted serine protease is tethered to the serpin via an ester bond formed between the catalytic serine hydroxyl group of the protease and the released carbonyl group at the C-terminus of the serpin cleaved at the active site (38). To determine whether miropin inhibits plasmin in the same manner, a constant amount of miropin was incubated with increasing plasmin concentrations. Afterwards, the proteins were subjected to SDS-PAGE analysis under reducing and non-reducing conditions. With increasing protease concentrations, the intensity of the band corresponding to miropin (~42 kDa) decreased with a simultaneous

increase in the intensity of new bands with higher molecular masses of ~60 kDa and ~120 kDa under reducing and non-reducing conditions, respectively (Fig. 3A). These new bands correspond to covalent complexes of miropin cleaved at the RCL (~37 341 kDa) and the light chain of plasmin (~24 kDa), and the light and heavy chains of plasmin linked by disulfide bridges (~80 kDa), respectively. To unambiguously confirm the apparent formation of a denaturation-stable covalent complex between miropin and plasmin, we performed mass spectrometry analysis. This experiment confirmed the presence of both miropin and plasmin in the bands assumed to contain complexes (Table 1).Finally, to identify the reactive site (i.e., the cleavage site within the miropin RCL) for plasmin inhibition, the 346 proteins in a reaction mixture of plasmin and miropin were resolved via SDS-PAGE and transferred to a PVDF 347 membrane. Next, the N-terminal sequence of a ~5 kDa peptide was determined via Edman degradation (Fig. 3B). As expected, plasmin attacked the miropin RCL at only one position, i.e., the Lys-Thr (P2-P1) peptide 349 bond, which corresponds exactly to the substrate specificity of plasmin.

Both *T. forsythia* cell-associated and OMV-released miropin can inhibit plasmin

Miropin is translated with a signal peptide that leads to its export to the periplasm via the Sec system (31, 39). To investigate the ability of miropin to interact with proteases in the extracellular environment, we preincubated plasmin with increasing amounts of washed *T. forsythia* cell suspension and OMVs, and then measured the residual activity. Both the cells and OMVs of the wild-type *T. forsythia* strain, but not those of its isogenic miropin-null mutant, inhibited plasmin in a concentration-dependent manner (Fig. 4A,B). As in the case of recombinant miropin, plasmin inhibition by intact cells and OMV-associated miropin occurred via covalent complex formation (Fig. 4C,D).

The linear decrease in the plasmin activity as a function of the cell suspension volume allowed titration of the miropin associated with intact bacteria cells and OMVs, which revealed that there were 640 copies of inhibitor per *T. forsythia* cell and 50 fmol per 1 μg protein in the OMV fraction. Importantly, the miropin-null mutant did not affect plasmin activity, arguing that *T. forsythia* does not express any other inhibitor capable of 364 inhibiting plasmin. Finally, the lack of any significant plasmin inhibition by non-concentrated culture medium 365 indicates that most of the miropin is associated with bacterial cells.

Miropin is the effective plasmin inhibitor in human plasma

In vivo, miropin interacts with human plasmin in gingival crevicular fluid (GCF) or in blood plasma (when *T. forsythia* penetrates into the circulation) in the presence of many other proteins, including proteolytic enzymes, zymogens, and protease inhibitors. Consequently, plasma proteins could interfere with the inhibitory activity of miropin against plasmin. Thus, to verify the ability of miropin to target plasmin in complex pathophysiological fluids, we titrated the effect of miropin on plasmin activity in whole human blood plasma in which plasminogen was converted to plasmin via preincubation with streptokinase. As shown in Fig. 5A, miropin inhibited plasmin activity in a concentration-dependent manner via formation of covalent inhibitory complexes (Fig. 5B). Of note, complexes were not detected in samples lacking streptokinase or containing inactive against plasmin miropin mutant,

miropin^{K368A}. The inhibition occurred with a k_{ass} of 1.1×10^3 M^{-1} s^{-1} (Fig. 5C), which is almost the same as value of k_{ass} (1.2×10^3 M^{-1} s^{-1}) determined under the same experimental conditions for α_2AP (data not shown).

To further investigate the potency of miropin to inhibit plasmin fibrinolytic activity *ex vivo*, thrombin-clotted human plasma was treated first with miropin or α_2AP and then with plasmin, and clot solubilization was recorded as a function of time. As shown in Fig. 5D, miropin prevented clot lysis in a concentration-dependent manner with an efficiency only slightly lower than that of α_2AP. To make a final comparison between the potencies of miropin and α_2AP to inhibit plasmin under pathophysiologically relevant conditions, we supplemented human α_2AP-deficient plasma with purified α_2AP or miropin at molar concentrations equivalent to the physiological concentration of α_2AP and used such plasma to inhibit plasmin. Supplementation with miropin significantly increased the potency of the inhibitory effect of plasma on plasmin to a level only slightly lower than that in α_2AP-supplemented sample. The inactive miropin variant (miropin^{K368A}) was used as a control, and it did not affect the inhibitory effect of plasma on plasmin beyond the inhibition level due to other plasmin inhibitors than α_2AP present in human plasma (Fig. 5E).

Collectively, our data showed that miropin, both *in vitro* and *ex vivo*, is a potent plasmin inhibitor with an efficiency comparable to that of α_2AP, the major physiological plasmin inhibitor.

Miropin reduces blood loss in mice and protects *T. forsythia* cell envelope proteins against plasmin

In periodontal pockets, subgingival dysbiotic microbial biofilms are immersed in a GCF consisting of ~70% 397 blood plasma and are exposed to the pro-clotting activity of gingipains (40), which is produced by *P. gingivalis*, 398 the major periodontal pathogen always found together with *T. forsythia* (41). By slowing the GCF flow and 399 trapping erythrocytes, local coagulation can be envisioned as being beneficial for the asaccharolytic *P. gingivalis*, which requires heme and peptides for its growth. In this context, inhibition of fibrinolysis by miropin could benefit the entire community of subgingival bacteria. To demonstrate miropin activity *in vivo*, we compared levels of blood loss from the excised tail veins of mice intravenously injected with miropin, aprotinin, or a vehicle, and we found that miropin reduced blood loss by 30% (Fig. 6A). At the same molar concentration, aprotinin, a plasmin inhibitor approved for the reduction of blood loss during major surgeries (42), prevented blood loss by 45%. Together, these findings confirmed that miropin is active in the blood and may reduce clot lysis in periodontal pockets.

The subcellular localization of miropin suggests that this serpin could protect cell envelope proteins against degradation by proteolytic enzymes, including plasmin. To verify this hypothesis, we incubated the CE fraction derived from the WT and Δmiropin *T. forsythia* strains with plasmin and found that the CE proteins of the WT cells were degraded at a significantly lower rate than those of the Δmiropin cells. Importantly, this protein degradation was prevented by external addition of native miropin but not miropin^{K368A} (Fig. 6B).

DISCUSSION

Plasminogen is the key component of the plasminogen activation system and is one of the proteins essential for homeostasis maintenance in the mouse periodontium (13). In humans, genetic (43) or induced (12) deficiencies in plasmin activity often (34% in congenital type I plasminogen deficiency) lead to ligneous conjunctivitis in most cases associated with periodontium destruction (ligneous periodontitis). Interestingly, spontaneous development of periodontitis in plasminogen-null and tPA/uPA double-deficient mice closely resembles the 420 pathological progression of the human disease (13). Furthermore, polymorphisms in the genes encoding uPA 421 and PAI-1 are associated with periodontal bone loss (44). These observations strongly suggest that plasmin activity is essential for periodontal health in humans. In this context, the discovery that *T. forsythia*, the major periodontal pathogen in humans, produces the very efficient serpin-type plasmin inhibitor miropin is fascinating.

Miropin inhibited human plasmin with an SI = 3.8 and a k_{ass} of 3.3×10^5 M^{-1} s^{-1}, while the same parameters for antiplasmin are 1.1 and 1.3×10^6 M^{-1} s^{-1}, respectively. Using 25-times higher plasmin concentration (1 μM) than in Fig. 2A decreased the value of SI to 2.3 (data not shown). Of note, miropin inhibits with SI higher than unity, in sharp contrast to the majority of described prokaryotic and human serpins, not only plasmin, but also all other target proteases (31,32). Detailed crystallographic analysis of both native and induced, cleaved by target proteases, miropin (32) could exclude the possibility that higher SI resulted from the fact that recombinant miropin used in the experiments had already undergone structural transition analogous to PAI-1 or been cleaved within RCL. Moreover, incubation of miropin with target proteases always yielded the inhibitor conversion to inhibitory complexes or the RCL cleaved form, which is a characteristic feature exclusive for native inhibitory serpins (31). Higher SI could also be explained by cleavage of miropin by plasmin at different positions than RSB, which will lead not to inhibition but inactivation of the serpin molecule. This hypothesis could be excluded by the observation that N-terminal sequencing revealed the presence of only a single sequence (Fig. 3B). This finding is also corroborated by the fact that miropin^{K368A}, mutant not inhibiting plasmin, was not cleaved at all by plasmin (data not shown). Apparently, it looks like that higher SI, together with possessing three equivalent RSBs (32), is a unique feature of miropin distinguishing it from other characterized serpins. The plasmin inhibition occurred via the formation of a stable covalent complex following proteolytic cleavage of the Lys368-Thr369 (P2-P1) RSB. A comparison of the RCL sequences of various serpins revealed that this site lies one residue upstream from the canonical RSB at P1-P1' that is used for protease inhibition by nearly all serpins. Of note, the P1-P1' RSB of miropin is used to inhibit subtilisin (31). Interestingly, a similar situation was described in the case of α_2-antiplasmin, in which the canonical RSB (Met365-Ser366) is used for chymotrypsin inhibition, while plasmin is inhibited at the P2-P1 RBS (Arg364-Met365). However, in stark contrast to α_2AP, miropin possesses a third RBS (Val367-Lys368) and inhibits neutrophil elastase, while antiplasmin is inactivated by this protease. Thus, it is possible that the lower k_{ass} for plasmin inhibition is an evolutionary price paid to possess the third RSB.

Miropin inhibited not only purified human plasmin but also substituted for the α_2AP inhibitory function in antiplasmin-deficient plasma; it also inhibited streptokinase-activated

plasminogen directly in human plasma and blocked degradation of fibrin clots. In all of these assays, the efficiencies of miropin were comparable to those of α_2AP, as only a 2-fold higher miropin concentration was required to match the α_2AP inhibitory performance. This property is apparently related to the lower k_{ass} values for plasmin inhibition by miropin relative to those of α_2AP. Furthermore, miropin was shown to be active *in vivo*, as it reduced blood loss in a mouse tail bleeding assay. Finally, and importantly in light of *in vivo* pathobiological interactions, both miropin associated with intact *T. forsythia* cells and that released into the environment on the surface of outer membrane vesicles were fully active against plasmin to the point that it was possible to titrate bacterial cell- and OMV-associated miropin. Apparently, high levels of miropin on the cell surface protect CE proteins of *T. forsythia*, from proteolytic degradation not only by plasmin, but also other proteases, especially neutrophil elastase.

Collectively, these data clearly show that miropin can interfere with plasmin activity at bleeding-prone *T. forsythia*-infected periodontitis sites soaked with GCF, which contains 70% blood plasma. The high *in vivo* expression of miropin at periodontitis sites (45) further argues that miropin may have significant effects on the pathobiological events during the initiation and progression of periodontitis. First, it can interfere directly with the main physiological functions of plasmin: to degrade fibrin in blood clots and fibrin deposits in periodontal tissue. Pathological fibrin deposits in plasmin activity-deficient mice (13) and in cases of ligneous periodontitis in humans (11) suggest that these activities of miropin would have deleterious effects. Second, inhibition of direct and indirect interactions between plasmin and the host immune response against pathogens may lead to detrimental effects on periodontal health. This role of plasmin was confirmed by the observation that *Staphylococcus aureus* clearance was impaired in mice lacking plasmin in comparison to the clearance in wild-type mice (46). Thus, miropin-mediated plasmin inhibition may result in protection not only of *T. forsythia* but also of other bacteria dwelling in the dental plaque against host immune defense mechanisms, which may be crucial especially during the initiation of periodontitis. Third, plasmin interacting with uPA and PAR-1 activates a pathway that attenuates inflammatory osteoclastogenesis in LPS-stimulated macrophages (47). Considering the heavy load of LPS-releasing Gram-negative bacteria in the periodontal pockets, inhibition of this pathway by miropin may contribute to alveolar bone resorption.

Considering the potential effects of miropin on the virulence of *T. forsythia*, we must keep in mind that *T. forsythia* is part of a complex microbiome in the subgingival dental plaque in which it exists in very close association with *P. gingivalis* (41). Interestingly, via its arginine-specific factor gingipain, *P. gingivalis* can 484 activate many factors in the coagulation cascade, including thrombin (40), thus leading to fibrin deposit 485 accumulation in the proximity of the biofilm. Plasmin-dependent degradation of fibrin meshes containing 486 entrapped erythrocytes may constitute a sustained source of peptides and heme for the entire bacterial community, but especially for *P. gingivalis*, whose proliferation depends on heme as an essential growth factor and peptides as a carbon and energy source. On the other hand, plasminogen capture and activation by periodontal pathogens such as *T. denticola* and *F. nucleatum*, which express plasminogen receptors, should create zones of increased peribacterial proteolytic activity that are spatially separated from *P. gingivalis* and *T. forsythia*, which occupy a different niche in the plaque (28, 48).

The above discussion illustrates a problem with assigning a virulence function to miropin, which might actually help to protect periodontal tissues from damage by plasmin-dependent host responses. Control of plasmin activity may prevent excessive activation of matrix metalloproteases (11), which can degrade the collagen in periodontal ligament fibers. *uPA*$^{-/-}$ mice are resistant to *P. gingivalis* oral gavage-induced periodontitis (49) via a macrophage-dependent mechanism (47). Apparently, the *P. gingivalis* gingipain complex potentiates matrix degradation by macrophages in a uPA- and plasmin activity-dependent manner. Therefore, it is tempting to speculate that periodontal plaques containing a higher number of *T. forsythia* cells than *P. gingivalis* cells may cause less damage.

Taken together, our results reveal miropin as the first bacterial proteinaceous plasmin inhibitor. It is produced by the periodontal pathogen *T. forsythia*, and its antiplasmin inhibitory efficiency is comparable to that of α_2AP, the main human plasmin inhibitor. Due to its secretory characteristics, miropin may contribute to the development of periodontitis by interfering with plasmin-mediated degradation of fibrin deposits in periodontal tissue in a similar manner as described for plasmin activity-deficient patients. Alternatively, miropin could interfere with plasmin functions in the immune system. Verification of the impact of miropin on the pathobiology of the periodontium requires additional mouse model studies, which are the focus of our ongoing research.

ACKNOWLEDGMENTS

This study was supported in part by grants UMO-2015/17/B/NZ1/00666 UMO-2016/21/B/NZ1/00292 from National Science Center (Krakow, Poland) and R21DE026280 from NIH/NIDCR. MK has obtained a scholarship from Ministry of Science and Higher Education (1306/MOB/IV/2015/0, “Mobilność Plus”).

ABBREVIATIONS:

α2AP	α2-antiplasmin
α2M	α2-macroglobulin
AMC	7-Amino-4-methylcoumarin
APTT	partial thromboplastin time
Boc	t-butoxycarbonyl
CE	cell envelope
GCF	gingival crevicular fluid
k_{ass}	the second-order association rate constant
K_M	the Michaelis-Menten constant
LPS	Lipopolisacharyd
OMVs	outer membrane vesicles
PAI-1/2	plasminogen activator inhibitor-1/2

PAR-1	protease-activated receptor-1
PT	prothrombin time
RCL	reactive center loop
RSB	reactive site bond
SD	standard deviation
SI	stoichiometry of inhibition
SK	streptokinase
tPA	tissue plasminogen activator
uPA	urokinase plasminogen activator
WCs	whole cells

REFERENCES

1. Castellino FJ, and Ploplis VA (2005) Structure and function of the plasminogen/plasmin system.Thromb. Haemost 93, 647–654 [PubMed: 15841308]
2. Krafts KP (2010) Tissue repair: The hidden drama. Organogenesis 6, 225–233 [PubMed: 21220961]
3. Cesarman-Maus G, and Hajjar KA (2005) Molecular mechanisms of fibrinolysis. Br. J. Haematol 129,307–321 [PubMed: 15842654]
4. Ulisse S, D'Armiento M, Bocchini S, and Baldini E. (2011) Plasminogen-Activating System. In 532 Encyclopedia of Cancer. (Schwab M, ed.) pp. 2904–2907, Springer, Berlin, Heidelberg
5. Neilands J, Bikker FJ, and Kinnby B. (2016) PAI-2/SerpinB2 inhibits proteolytic activity in a P.gingivalis-dominated multispecies bacterial consortium. Arch. Oral. Biol 70, 1–8 [PubMed: 27295389]
6. Collen D. (1980) Natural inhibitors of fibrinolysis. J. Clin. Pathol. Suppl. (R. Coll. Pathol) 14, 24–30 [PubMed: 6448870]
7. Peetermans M, Vanassche T, Liesenborghs L, Lijnen RH, and Verhamme P. (2016) Bacterial pathogens activate plasminogen to breach tissue barriers and escape from innate immunity. Crit. Rev. Microbiol 42, 866–882 [PubMed: 26485450]
8. Liesenborghs L, Verhamme P, and Vanassche T. (2018) Staphylococcus aureus, master manipulator of 540 the human hemostatic system. J. Thromb. Haemost 16, 441–454 [PubMed: 29251820]
9. Lähteenmäki K, Kuusela P, and Korhonen TK (2011) Bacterial plasminogen activators and receptors.FEMS Microbiol. Rev 25, 531–552
10. Celkan T. (2017) Plasminogen deficiency. J Thromb Thrombolysis. 43, 132–138 [PubMed: 27629020]
11. Kurtulus Waschulewski I, Gökbuget AY, Christiansen NM, Ziegler M, Schuster V, Wahl G, and Götz W. (2016) Immunohistochemical analysis of the gingiva with periodontitis of type I plasminogendeficiency compared to gingiva with gingivitis and periodontitis and healthy gingiva. Arch. Oral. Biol 72, 75–86 [PubMed: 27552374]
12. Scully C, Gokbuget AY, Allen C, Bagan JV, Efeoglu A, Erseven G, Flaitz C, Cintan S, Hodgson T, Porter SR, and Speight P. (2001). Oral lesions indicative of plasminogen deficiency (hypoplasminogenemia). Oral Surg. Oral Med. Oral Pathol. Oral Radiol. Endod 91, 334–337 [PubMed: 11250632]
13. Sulniute R, Lindh T, Wilczynska M, Li J, and Ny T. (2011) Plasmin is essential in preventing periodontitis in mice. Am. J. Pathol 179, 819–828 [PubMed: 21704601]

14. Nazir MA (2017) Prevalence of periodontal disease, its association with systemic diseases and prevention. Int. J. Health Sci. (Qassim) 11, 72–80 [PubMed: 28539867]
15. Suzuki J, Aoyama N, Ogawa M, Hirata Y, Izumi Y, Nagai R, and Isobe M. (2010) Periodontitis andcardiovascular diseases. Expert Opin. Ther. Targets 14, 1023–1027 [PubMed: 20678026]
16. Persson RE, Hollender LG, MacEntee MI, Wyatt CCL, Kiyak HA, and Persson GR (2003) Assessment of periodontal conditions and systemic disease in older subjects. J. Clin. Periodontol 30, 207–213 [PubMed: 12631178]
17. Preshaw PM, Alba AL, Herrera D, Jepsen S, Konstantinidis A, Makrilakis K, and Taylor R. (2012) Periodontitis and diabetes: a two-way relationship. Diabetologia 55, 21–31 [PubMed: 22057194]
18. Srinivas SK, and Parry S. (2012) Periodontal disease and pregnancy outcomes: time to move on? J. Women's Heal 21, 121–125.
19. Ioannidou E, Swede H, and Dongari-Bagtzoglou A. (2011) Periodontitis predicts elevated C-reactiveprotein levels in chronic kidney disease. J. Dent. Res 90, 1411–1415 [PubMed: 21940520]
20. Benedyk M, Mydel P, Delaleu N, Płaza K, Gawron K, Milewska A, Maresz K, Koziel J, Pyrc K, and Potempa J. (2016) Gingipains: critical factors in the development of aspiration pneumonia caused by Porphyromonas gingivalis. J. Innate Immun 8, 185–198 [PubMed: 26613585]
21. Zeng X-T, Tu M-L, Liu D-Y, Zheng D, Zhang J, and Leng W. (2012) Periodontal Disease and Riskof Chronic Obstructive Pulmonary Disease: A Meta-Analysis of Observational Studies. PLoS One 7, e46508
22. Potempa J, Mydel P, and Koziel J. (2017) The case for periodontitis in the pathogenesis of rheumatoid arthritis. Nat. Rev. Rheumatol 13, 606–620 [PubMed: 28835673]
23. Dominy SS, Lynch C, Ermini F, Benedyk M, Marczyk A, Konradi A, Nguyen M, Haditsch U, Raha D,Griffin C, Holsinger LJ, Arastu-Kapur S, Kaba S, Lee A, Ryder MI, Potempa B, Mydel P, Hellvard A, Adamowicz K, Hasturk H, Walker GD, Reynolds EC, Faull RLM, Curtis MA, Dragunow M, and Potempa J. (2019) Porphyromonas gingivalis in Alzheimer's disease brains: Evidence for disease causation and treatment with small-molecule inhibitors. Sci. Adv 5, eaau3333
24. Socransky SS, Haffajee AD, Cugini MA, Smith C, and Kent RL (1998) Microbial complexes insubgingival plaque. J. Clin. Periodontol 25, 134–144 [PubMed: 9495612]
25. Hajishengallis G, and Lamont RJ (2012) Beyond the red complex and into more complexity: thepolymicrobial synergy and dysbiosis (PSD) model of periodontal disease etiology. Mol. Oral. Microbiol 27, 409–419 [PubMed: 23134607]
26. Cortés-Vieyra R, Rosales C, and Uribe-Querol E. (2016) Neutrophil functions in periodontal homeostasis. J. Immunol. Res 2016, 1396106 [PubMed: 27019855]
27. Hienz SA, Paliwal S, and Ivanovski S. (2015) Mechanisms of bone resorption in periodontitis. J. Immunol. Res 2015, 615486 [PubMed: 26065002]
28. Vieira ML, and Nascimento AL (2016) Interaction of spirochetes with the host fibrinolytic system and potential roles in pathogenesis. Crit. Rev. Microbiol 42, 573–587 [PubMed: 25914944]
29. Ksiazek M, Mizgalska D, Eick S, Thøgersen IB, Enghild JJ, and Potempa J. (2015) KLIKK proteases of Tannerella forsythia: putative virulence factors with a unique domain structure. Front. Microbiol 6, 312 [PubMed: 25954253]
30. Potempa J, and Pike RN (2009) Corruption of innate immunity by bacterial proteases. J. Innate Immun 1, 70–87 [PubMed: 19756242]
31. Ksiazek M, Mizgalska D, Enghild JJ, Scavenius C, Thogersen IB, and Potempa J. (2015) Miropin, a novel bacterial serpin from the periodontopathogen Tannerella forsythia, inhibits a broad range of proteases by using different peptide bonds within the reactive center loop. J. Biol. Chem 290, 658–670 [PubMed: 25389290]
32. Goulas T, Ksiazek M, Garcia-Ferrer I, Sochaj-Gregorczyk AM, Waligorska I, Wasylewski M, Potempa J, and Gomis-Rüth FX (2017) A structure-derived snap-trap mechanism of a multispecific serpin from the dysbiotic human oral microbiome. J. Biol. Chem 292, 10883–10898 [PubMed: 28512127]
33. Lasica AM, Goulas T, Mizgalska D, Zhou X, de Diego I, Ksiazek M, Madej M, Guo Y, Guevara T, Nowak M, Potempa B, Goel A, Sztukowska M, Prabhakar AT, Bzowska M, Widziolek M, Thøgersen IB, Enghild JJ, Simonian M, Kulczyk AW, Nguyen KA, Potempa J, and Gomis-Rüth FX (2016) Structural and functional probing of PorZ, an essential bacterial surface component of

the type-IX secretion system of human oral-microbiomic Porphyromonas gingivalis. Sci. Rep 6, 37708 [PubMed: 27883039]

34. Friedrich V, Gruber C, Nimeth I, Pabinger S, Sekot G, Posch G, Altmann F, Messner P, Andrukhov O, and Schäffer C. (2015) Outer membrane vesicles of Tannerella forsythia: biogenesis, composition, and virulence. Mol. Oral Microbiol 30, 451–473 [PubMed: 25953484]
35. Schägger H, and von Jagow G. (1987) Tricine-sodium dodecyl sulfate-polyacrylamide gel electrophoresis for the separation of proteins in the range from 1 to 100 kDa. Anal. Biochem 166, 368–379 [PubMed: 2449095]
36. Braun V, and Rehn K. (1969) Chemical characterization, spatial distribution and function of a lipoprotein (murein-lipoprotein) of the E. coli cell wall. The specific effect of trypsin on the membrane structure. Eur. J. Biochem 10, 426–438 [PubMed: 4899922]
37. Uete T, Shimano N, and Morikawa M. (1975) Simple, sensitive method for measuring plasmin and plasminogen activity in plasma. Clin. Chem 21, 1632–1637 [PubMed: 240516]
38. Huntington JA, Read RJ, and Carrell RW (2000) Structure of a serpin–protease complex shows inhibition by deformation. Nature 407, 923–936 [PubMed: 11057674]
39. Almagro Armenteros JJ, Tsirigos KD, Sønderby CK, Petersen TN, Winther O, Brunak S, vonHeijne G, and Nielsen H. (2019) SignalP 5.0 improves signal peptide predictions using deep neural networks. Nat. Biotechnol 37, 420–423 [PubMed: 30778233]
40. Imamura T, Banbula A, Pereira PJ, Travis J, and Potempa J. (2001) Activation of human prothrombinby arginine-specific cysteine proteinases (Gingipains R) from Porphyromonas gingivalis. J. Biol. Chem 276, 18984–18991 [PubMed: 11278315]
41. Wara-aswapati N, Pitiphat W, Chanchaimongkon L, Taweechaisupapong S, Boch JA, Ishikawa I(2009) Red bacterial complex is associated with the severity of chronic periodontitis in a Thai population. Oral Dis. 15, 354–359 [PubMed: 19371397]
42. Khoshhal K, Mukhtar I, Clark P, Jarvis J, Letts M, and Splinter W. (2003) Efficacy of aprotinin in reducing blood loss in spinal fusion for idiopathic scoliosis. J. Pediatr. Orthop 23, 661–664 [PubMed: 12960633]
43. Tefs K, Gueorguieva M, Klammt J, Allen CM, Aktas D, Anlar FY, Aydogdu SD, Brown D, Ciftci E, Contarini P, Dempfle CE, Dostalek M, Eisert S, Gökbuget A, Günhan O, Hidayat AA, Hügle B, Isikoglu M, Irkec M, Joss SK, Klebe S, Kneppo C, Kurtulus I, Mehta RP, Ornek K, Schneppenheim R, Seregard S, Sweeney E, Turtschi S, Veres G, Zeitler P, Ziegler M, and Schuster V. (2006) Molecular and clinical spectrum of type I plasminogen deficiency: a series of 50 patients. Blood 108, 3021–3026 [PubMed: 16849641]
44. DeCarlo AA, Grenett H, Park J, Balton W, Cohen J, and Hardigan P. (2007) Association of genepolymorphisms for plasminogen activators with alveolar bone loss. J. Periodontal. Res 42, 305–310 [PubMed: 17559626]
45. Eckert M, Mizgalska D, Sculean A, Potempa J, Stavropoulos A, and Eick S. (2018) In vivo expression of proteases and protease inhibitor, a serpin, by periodontal pathogens at teeth and implants. Mol. Oral. Microbiol 33, 240–248 [PubMed: 29498485]
46. Guo Y, Li J, Hagström E, and Ny T. (2008) Protective effects of plasmin(ogen) in a mouse model ofStaphylococcus aureus–induced arthritis. Arthritis Rheum. 58, 764–772 [PubMed: 18311818]
47. Kanno Y, Ishisaki A, Kawashita E, Kuretake H, Ikeda K, and Matsuo O. (2016) uPA attenuated LPS-induced inflammatory osteoclastogenesis through the Plasmin/PAR-1/Ca(2+)/CaMKK/AMPK axis. Int. J. Biol. Sci 12, 63–71 [PubMed: 26722218]
48. Darenfed H, Grenier D, and Mayrand D. (1999) Acquisition of plasmin activity by Fusobacterium nucleatum subsp. nucleatum and potential contribution to tissue destruction during periodontitis. Infect. Immun 67, 6439–6444 [PubMed: 10569761]
49. Lam RS, O'Brien-Simpson NM, Hamilton JA, Lenzo JC, Holden JA, Brammar GC, Orth RK, Tan Y, Walsh KA, Fleetwood AJ, and Reynolds EC. (2015) GM-CSF and uPA are required for Porphyromonas gingivalis-induced alveolar bone loss in a mouse periodontitis model. Immunol. Cell Biol93, 705–715 [PubMed: 25753270]

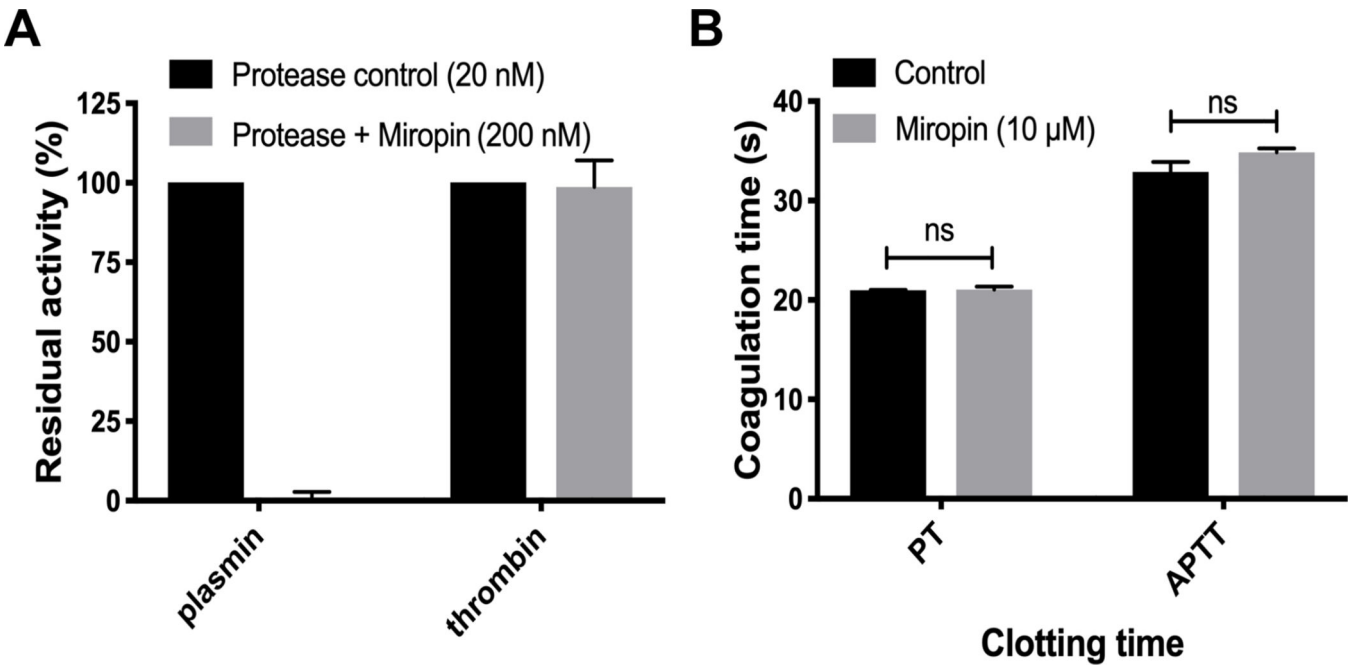

Figure 1:

Miropin inhibits plasmin but not coagulation cascade proteases. A) Human plasmin and thrombin were incubated with a 10-molar excess of miropin, and their residual activitieswere determined. B) Plasma was preincubated with miropin, and the prothrombin time (PT) and activated partial thromboplastin time (APTT) were evaluated using a C-2 dual channel coagulometer. In both panels, the data shown are the means and standard deviations of the means from three replicates.

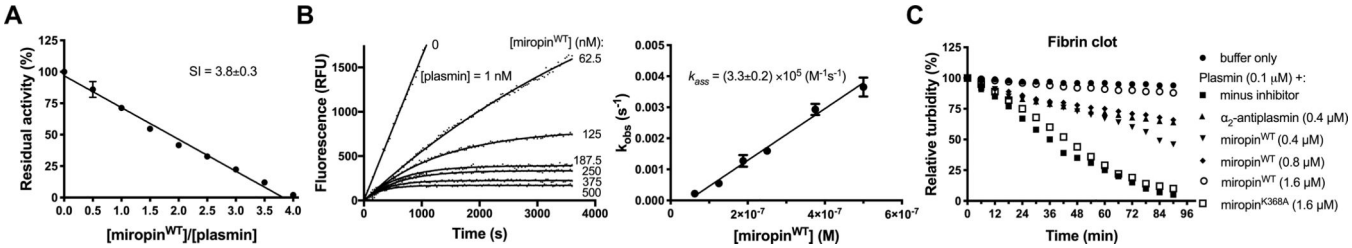

Figure 2:

Miropin is an efficient inhibitor of human plasmin as indicated by its stoichiometry of inhibition (SI) (A), association rate constant (k_{ass}) (B), and ability to inhibit the fibrinolytic activity of plasmin (C). A) Plasmin was preincubated with increasing miropin concentrations for 15 min, and the residual enzymaticactivity was measured and plotted against the miropin:plasmin molar ratio. B) Plasmin was added to mixtures 6 containing a constant amount of substrate and increasing miropin concentrations. Changes in fluorescence (RFU) were then recorded. Based on progress curve analysis, the k_{obs} values were plotted as a function of the miropin concentration, and the k_{ass} was determined from the slope of the linear curve fit to the data points and corrected for the stoichiometry factor and K_M. C) α_2AP and miropin were added to thrombin-induced fibrin mesh, and the plasmin-mediated clot degradation was monitored by measuring the absorbance at 350 nm. The miropin K368A mutant (miropin^{K368A}), which is inactive against plasmin, was used as a control. The results presented (A, B) are the mean ± SD.

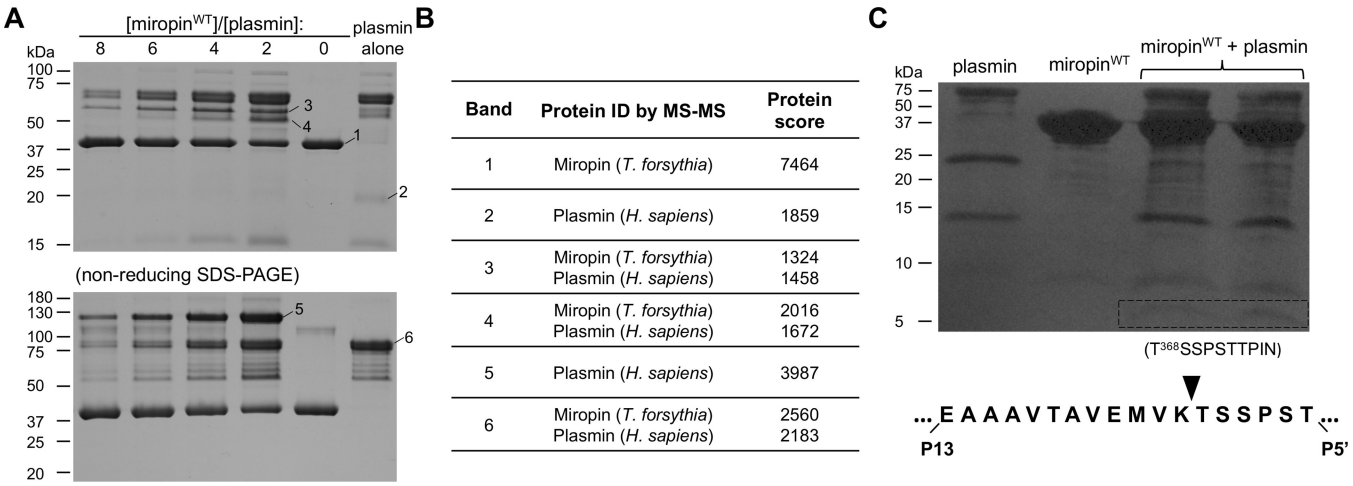

Band	Protein ID by MS-MS	Protein score
1	Miropin (*T. forsythia*)	7464
2	Plasmin (*H. sapiens*)	1859
3	Miropin (*T. forsythia*) Plasmin (*H. sapiens*)	1324 1458
4	Miropin (*T. forsythia*) Plasmin (*H. sapiens*)	2016 1672
5	Plasmin (*H. sapiens*)	3987
6	Miropin (*T. forsythia*) Plasmin (*H. sapiens*)	2560 2183

Figure 3:

Miropin forms stable covalent complexes after cleavage of the Lys^{368}(P2)-Ala(P1) reactive site 675 peptide bond. A) The protease and inhibitor were incubated together at different molar ratios or alone, and then separated by SDS-PAGE under reducing (upper gel) and non-reducing (lower gel) conditions. Selected bands were excised and subjected to mass spectrometry analysis to identify the proteins in the bands (Table 1). B) Miropin was incubated with plasmin until the reaction was stopped via addition of reducing sample buffer. The proteins were then resolved via SDS-PAGE and electrotransferred onto a PVDF membrane. The stained protein bands with a molecular weight of ~5 kDa (framed) were excised and subjected to N-terminal sequence analysis, which allowed identification of the RBS, K^{368} (P2)-Ala (P1), for plasmin within the miropin reactive center loop.

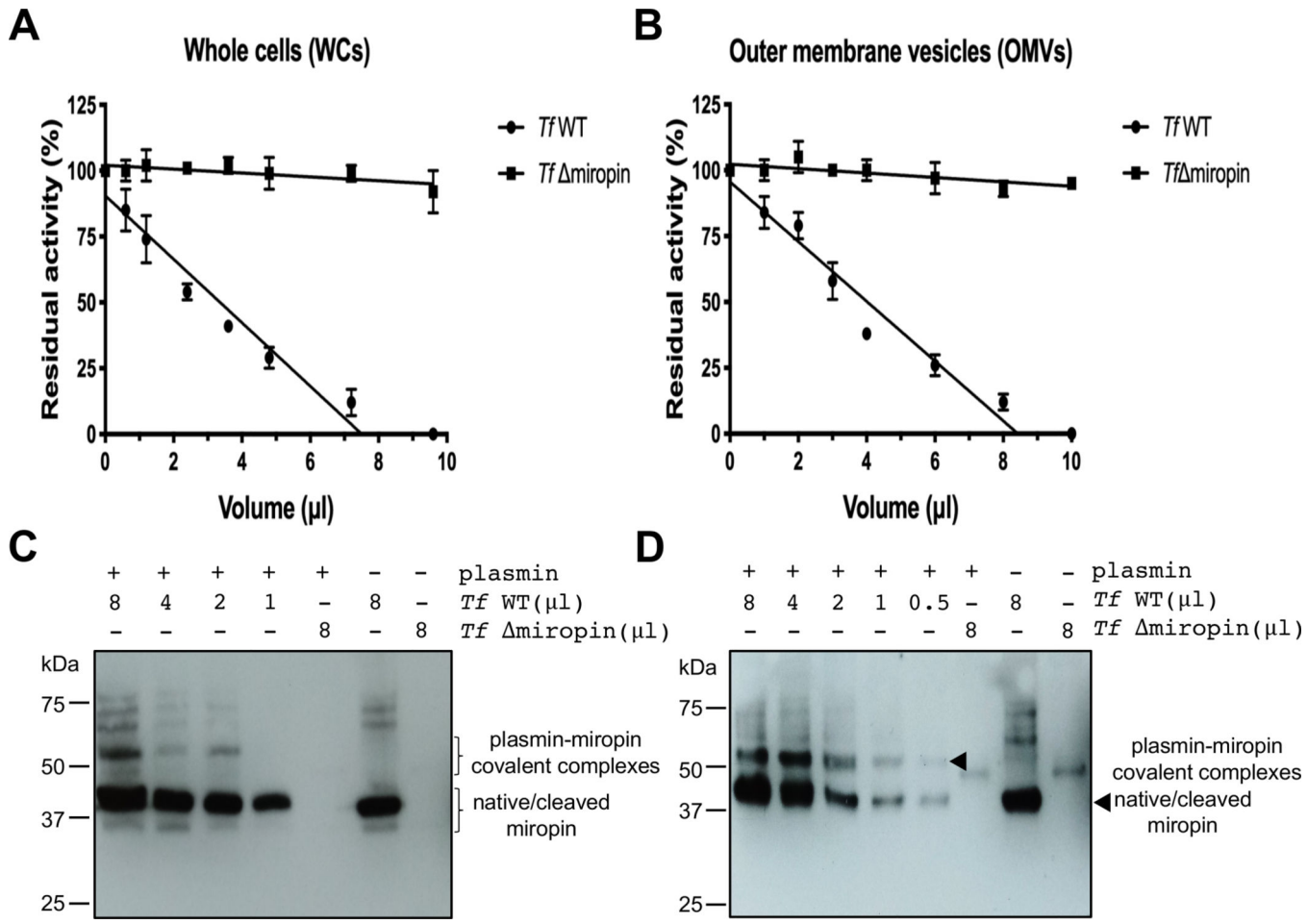

Figure 4:

Plasmin is inhibited by whole, intact *T. forsythia* cells and by outer membrane vesicles (OMVs) Increasing volumes of suspensions of whole cells (A, B) and OMVs (B, D) from wild-type and miropin-null 686 *T. forsythia* strains were added to human plasmin in microtitration plates. Residual plasmin activity was measured by employing Boc-QAR-AMC as a substrate (A, B). Covalent complex formation was verified via 688 Western blotting with anti-miropin antibodies (C, D). The data shown are the means and standard deviations of 689 the means from three replicates.

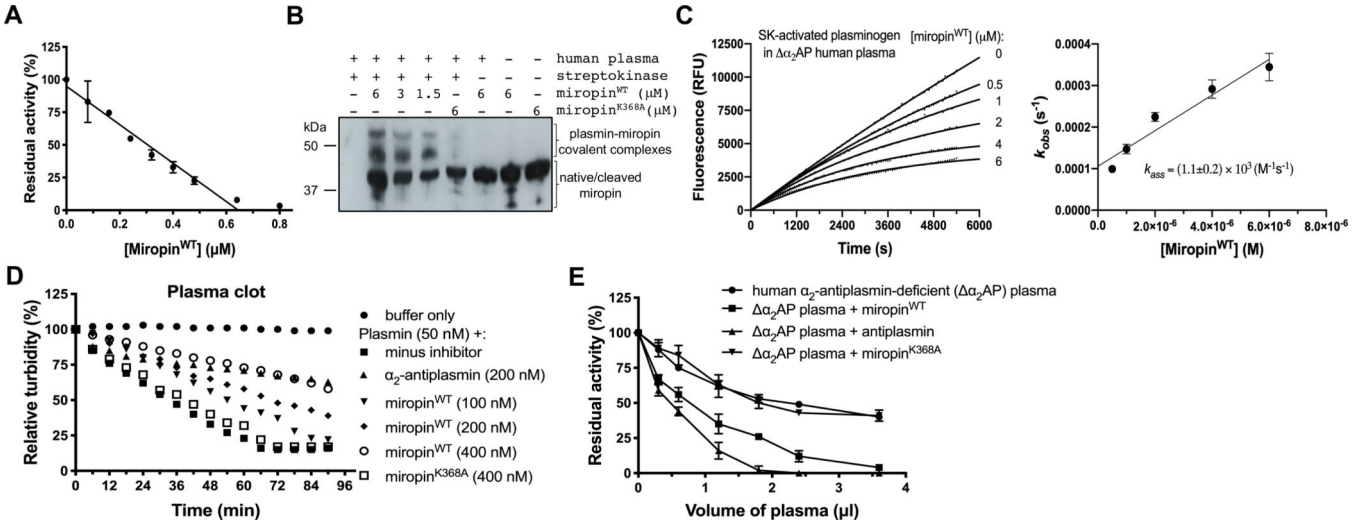

Figure 5:

Miropin is the effective plasmin inhibitor under *ex vivo* conditions A) Human plasma was treated with SK and then incubated with increasing miropin concentrations. Residual plasmin activity was measured using fibrinogen as a substrate, and (B) the formation of covalent complexes was verified via Western blotting with anti-miropin antibodies. In panel A, the mean ± SD from three experiments is presented. C) Determination of the k_{ass} for the inhibition of SK-activated plasminogen in human α_2AP-deficient plasma ($\Delta\alpha_2$AP) by miropin using inhibition progress curve analysis. D) Miropin was added to coagulated plasma at two different concentrations followed by plasmin addition, and the time-dependent clot degradation was monitored by measuring the absorbance at 350 nm. E) Human $\Delta\alpha_2$AP plasma was supplemented with 1 μM miropin, and increasing volumes of the supplemented plasma were then incubated with plasmin. The plasmin residual activity was measured using fluorogenic substrates (Boc-QAR-AMC). In all experiments, where indicated, α_2AP and miropin K368A were used as positive and negative controls, respectively.

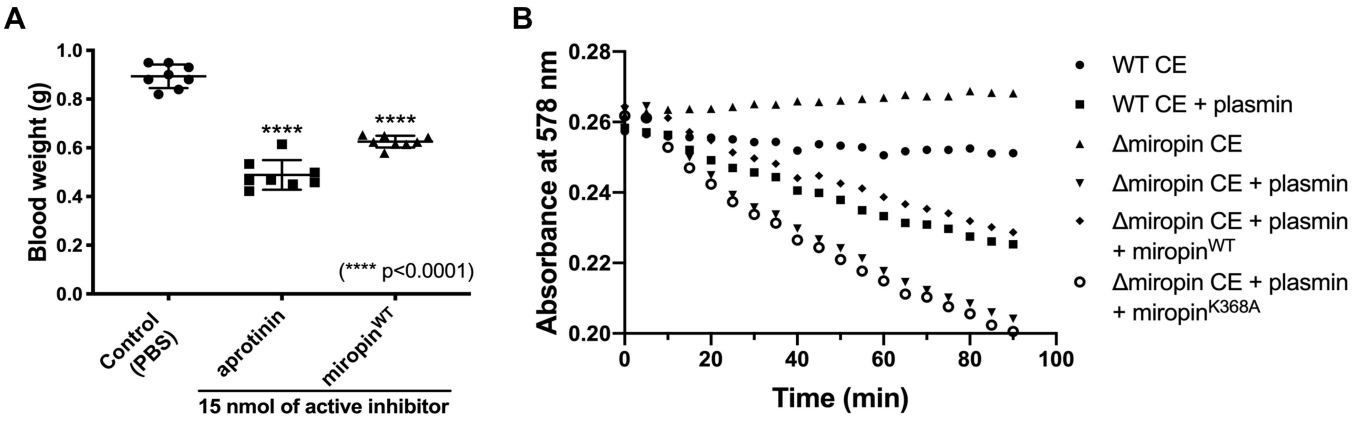

Figure 6:

Miropin reduces blood loss in a mouse tail bleeding model and protects *T. forsythia* cell envelope (CE) proteins against degradation by human plasmin. A) Under anesthesia, mice were intravenously injected (tail vein) with 100 µl PBS alone (control) or PBS containing 15 nmol bovine aprotinin or miropin. After 2 min, the tails were excised, and the blood was collected and weighed. The results presented as the mean ± SD (N = 8). B) The cell envelope (CE) fraction containing the inner and outer membranes and peptidoglycan were isolated from *T. forsythia* wild-type (WT) and Δmiropin mutant cells, and incubated with human plasmin. Protein degradation was monitored via measurement of the absorbance at 578 nm. To compensate for the missing inhibitory activity in the CE fraction from the *T. forshythia* Δmiropin mutant strain, either recombinant native miropin or the K368A antiplasmin-inactive variant was added prior to plasmin treatment.

Table 1:

Results from mass spectrometry analysis of putative complexes of miropin with plasmin.
The table shows the names of matched proteins and protein score. The protein score is the best total MS/MS 718 score obtained for the indicated protein by LC-MALDI of SDS-PAGE bands (Fig. 3A).

Band	Protein ID by MS-MS	Protein score
1	Miropin (*T. forsythia*)	7464
2	Plasmin (*H. sapiens*)	1859
3	Miropin (*T. forsythia*) Plasmin (*H. sapiens*)	1324 1458
4	Miropin (*T. forsythia*) Plasmin (*H. sapiens*)	2016 1672
5	Miropin (*T. forsythia*) Plasmin (*H. sapiens*)	2560 2183
6	Plasmin (*H. sapiens*)	3987